

Cosmological Simulation of Gravitational Weak Lensing in Open Models

Kenji TOMITA

Yukawa Institute for Theoretical Physics, Kyoto University, Kyoto 606-8502

Cosmological simulation of gravitational weak lensing in open models with $(\Omega_0, \lambda_0) = (0.2, 0)$ and $(0.4, 0)$ is treated using the direct integration method, which is independent of the multi-lens-plane method. Statistical averages of optical quantities (the convergence, shear, and amplification) are derived for ray bundles passing through the clumpy universe, in which the initial state has the CDM spectrum with the power $n = 1$, and all particles are regarded as equivalent (compact) lens objects with a galactic size. The compact lens objects consist of galaxies and dark matter particles. The evolution of the spatial mass distribution is given by N -body simulations in a tree-code. This paper is an extension of our previous one in flat models. The behaviors of optical quantities are shown in comparison with a low-density flat model with $(0.2, 0.8)$. It is found as a result that (1) optical quantities in the open model increase with Ω_0 , and (2) they are larger than those in the flat model with the same Ω_0 , and the difference is comparable with that between two open models with $\Omega_0 = 0.2$ and 0.4 . The comparison of the optical quantities with the corresponding observed ones will give us some information on the observational value of Ω_0 .

§1. Introduction

Gravitational weak lensing is one of the most useful tools for probing the inhomogeneous distribution of mass in the universe. The small deformation in the shape of distant galaxies caused by gravitational tidal force is directly connected with the total mass distribution in the neighbourhood of light paths to galaxies. Recently theoretical and observational studies on the deformed images of distant galaxies^{1) - 3)} have shown that in a near future the lensing information on the mass distribution brought with large telescopes will be useful to put severe constraints on dark matter, dark halos and allowed values of cosmological parameters.

In a previous paper⁴⁾ we treated the statistics of gravitational weak lensing in flat cosmological models in the direct integration method, in which the ray shooting was performed by solving null-geodesic equations numerically in the intervals between an observer and sources. Here weak lensing does not mean the weakest limit of lensing, but means that we treat only rays without caustics.

In this paper we extend the treatment to the case of open models and derive the average values of optical quantities on various angular scales, in comparison with those in the flat case. The largest difference of treatments in curved cases from the flat cases is that in curved cases we can construct no model universes covered everywhere with periodic boxes, and so, for the calculation of the gravitational forces from particles, we must assume a set of periodic boxes which are closely connected only along each light ray.

In §2 we show treated model universes and the equations for ray shooting in open models, and in §3 derive the statistical averages of optical quantities. Their

behaviors are shown in connection with those of the angular diameter distances. In §4 the comparison of average optical quantities with observed ones is discussed for the estimate of Ω_0 . In Appendices A the derivation of null-geodesic equations is shown in open models.

§2. Model universes and the ray shooting

The background model universes are assumed to be spatially open or have the negative curvature, and the behavior of light rays passing through inhomogeneities in them is considered at the stage from an initial time t_1 (with redshift $z_1 = 5$) to the present time t_0 . In the Newtonian approximation, the line-element is expressed as

$$ds^2 = -(1 + 2\varphi/c^2)c^2 dt^2 + (1 - 2\varphi/c^2)a^2(t)(d\mathbf{x})^2/[1 + K\frac{1}{4}(\mathbf{x})^2]^2, \quad (2.1)$$

where K is the signature of spatial curvature ($\pm 1, 0$). In the following we take $K = -1$. The normalized scale factor $S \equiv a(t)/a(t_0)$ satisfies

$$\left(\frac{dS}{d\tau}\right)^2 = \frac{1}{S} \left[\Omega_0 - (\Omega_0 + \lambda_0 - 1)S + \lambda_0 S^3 \right], \quad (2.2)$$

where $\tau \equiv H_0 t$ and $a_0 (\equiv a(t_0))$ is specified by a relation $(cH_0^{-1}/a_0)^2 = 1 - \Omega_0 - \lambda_0$. The gravitational potential φ is described by the Poisson equation

$$\begin{aligned} a^{-2} \Delta \varphi &= \left[1 - \frac{1}{4}(\mathbf{x})^2 \right]^2 \left[\frac{\partial^2 \varphi}{\partial \mathbf{x}^2} + \frac{\frac{1}{2}x^i}{\left[1 - \frac{1}{4}(\mathbf{x})^2 \right]^3} \frac{\partial \varphi}{\partial x^i} \right] \\ &= 4\pi G \rho_B [\rho(\mathbf{x})/\rho_B - 1], \end{aligned} \quad (2.3)$$

where $\rho_B (= \rho_{B0}/S^3)$ is the background density and

$$\rho_{B0} = \frac{3H_0^2 \Omega_0}{8\pi G} = 2.77 \times 10^{11} \Omega_0 h^2 M_\odot \text{ Mpc}^{-3}, \quad (2.4)$$

where $H_0 = 100h \text{ Mpc}^{-1} \text{ km s}^{-1}$. In our treatment the inhomogeneities are locally periodic in the sense that the physical situation at \mathbf{x} is the same as that at $\mathbf{x} + l\mathbf{n}$, where the components of $\mathbf{n} (= (n^1, n^2, n^3))$ are integers. In an arbitrary periodic box with coordinate volume l^3 , there are N particles with the same mass m . It is assumed that the force at an arbitrary point is the sum of forces from N particles in the box whose center is the point in question, and that the forces from outside the box can be neglected.

In this paper we take two open models (O1 model and O2 model) with $(\Omega_0, \lambda_0) = (0.2, 0)$ and $(0.4, 0)$, respectively, and a flat model (L model) with $(0.2, 0.8)$ for comparison. The present lengths of the boxes are

$$L_0 \equiv a(t_0)l = 50h^{-1}, 39.7h^{-1} \text{ Mpc} \quad (2.5)$$

for $\Omega_0 = 0.2, 0.4$, respectively. The particle number is 32^3 in both models, and so

$$m (= \rho_{B0} L_0^3 / N) = 2.11 \times 10^{11} h^{-1} M_\odot. \quad (2.6)$$

The distributions of particles in these models were derived by the numerical N -body simulations using Suto's tree-code⁵⁾ during the time interval $z = 0$ and $z = z_1$, where $z_1 = 5.0$ for all models. All particles in these models are regarded as equivalent (compact) lens objects with a galactic size, which consist of galaxies and dark matter.

For the compact lens objects we assume the physical softening radius $a(t)x_s = 20h^{-1}\text{kpc}$.

Light propagation is described by solving the null geodesic equation with the null condition. Here let us use $T \equiv \frac{1}{2} \ln[a(t)/a(t_1)]$ as a time variable and $T_0 \equiv (T)_{t=t_0}$. Then we have $dS = 2 \exp[2(T - T_0)]dT$, so that

$$cdt = R c_R [\Omega_0 + (1 - \Omega_0 - \lambda_0)S + \lambda_0 S^3]^{-1/2} e^{3T} dT, \quad (2.7)$$

where

$$R \equiv L_0 / [(1 + z_1)N^{1/3}] \quad (2.8)$$

and

$$c_R \equiv 2(c/H_0) / [R(1 + z_1)^{3/2}]. \quad (2.9)$$

The line-element is

$$ds^2/R^2 = -c_R^2 [\Omega_0 + (1 - \Omega_0 - \lambda_0)S + \lambda_0 S^3]^{-1} e^{6T} (1 + \alpha\phi) dT^2 + (1 - \alpha\phi) e^{4T} d\mathbf{y}^2 / F(\mathbf{y})^2, \quad (2.10)$$

where $y^0 = T$, $y^i = a(t_1)x^i/R$, $\varphi = (Gm/R)\phi$, $R_0 \equiv Ra_0/a_1 = (1 + z_1)R$,

$$\alpha \equiv \frac{2Gm}{c^2 R} = \frac{3}{\pi} \frac{\Omega_0}{(c_R)^2}, \quad (2.11)$$

and

$$F \equiv 1 - \frac{1}{4} (R_0 H_0 / c)^2 (1 - \Omega_0 - \lambda_0) (\mathbf{y})^2. \quad (2.12)$$

The equations for light rays to be solved are

$$\frac{dy^i}{dT} = c_R e^T \tilde{K}^i, \quad (2.13)$$

$$\begin{aligned} \frac{d\tilde{K}^i}{dT} = & -[3\lambda_0 e^{4(T-T_0)} + (1 - \Omega_0 - \lambda_0)] e^{2(T-T_0)} \tilde{K}^i / G(T) + \alpha \frac{\partial \phi}{\partial T} \tilde{K}^i \\ & - \gamma c_R^{-1} e^T \left[\partial \phi / \partial y^i / G(T) - 2 \frac{\partial \phi}{\partial y^j} \tilde{K}^j \tilde{K}^i \right] \\ & + (R_0 H_0 / c)^2 (1 - \Omega_0 - \lambda_0) F^{-1} c_R e^T \left[-y^j \tilde{K}^j \tilde{K}^i \right. \\ & \left. + \frac{1}{2} (1 + 2\alpha\phi) / G(T) \right], \end{aligned} \quad (2.14)$$

where $\gamma \equiv \alpha(c_R)^2$ and

$$G(T) = \Omega_0 + (1 - \Omega_0 - \lambda_0) e^{2(T-T_0)} + \lambda_0 e^{6(T-T_0)}. \quad (2.15)$$

The null condition is

$$\sum_i (\tilde{K}^i)^2 = 1 + 2\alpha\phi. \quad (2.16)$$

The derivation of these equations is given in Appendix A.

The potential ϕ is given as a solution of the Poisson equation. Because the ratio of the second term to the first term in the right-hand side of Eq. (2.3) is $(R_0 H_0 / c)^2 (\mathbf{y})^2 [\Delta y / |\mathbf{y}|] \ll 1$ for $z \leq z_1$, the Poisson equation in a box can be approximately expressed as

$$F(\mathbf{y}_c)^2 \frac{\partial^2 \phi}{\partial \mathbf{y}^2} = 4\pi G \rho_B [\rho(\mathbf{x}) / \rho_B - 1], \quad (2.17)$$

where we used that $F(\mathbf{y}) \simeq 1$ for $y \sim$ the box size and can be approximately replaced by the central value $F(\mathbf{y}_c)$ for $y \gg$ the box size and the suffix c denotes the central value in the box. For point sources with $\rho = m \sum_n \delta(aR(\mathbf{y} - \mathbf{y}_n))$ (n is the particle number), we have $\phi = \phi_1 + \phi_2$, where

$$\phi_1 = -F(\mathbf{y}_c) e^{-2T} \sum_n \frac{1}{|\mathbf{y} - \mathbf{y}_n|}, \quad (2.18)$$

and ϕ_2 displays the contribution from the homogeneous background density. Here let us use for \mathbf{y} another coordinates $\bar{\mathbf{y}}$ expressing the space in a locally flat way, where the two coordinates are connected as

$$\bar{\mathbf{y}} = \int_0^{\mathbf{y}} d\mathbf{y} / F(\mathbf{y}), \quad (2.19)$$

and the lengths between two points in boxes in two coordinates are approximately related as

$$\Delta \bar{\mathbf{y}} = \Delta \mathbf{y} / F(\mathbf{y}_c). \quad (2.20)$$

Then ϕ_1 is expressed in terms of $\bar{\mathbf{y}}$ in the usual manner as

$$\phi_1 = -e^{-2T} \sum_n \frac{1}{|\bar{\mathbf{y}} - \bar{\mathbf{y}}_n|}. \quad (2.21)$$

Corresponding forces are expressed as $f_i \equiv \partial \phi_1 / \partial y^i = [\partial \phi_1 / \partial \bar{y}^i] / F(\mathbf{y}_c)$. It should be noted that the contribution of $\partial \phi / \partial T$ is negligibly small, compared with that of f_i .

In flat models the universe is everywhere covered with periodic boxes continuously connected as in Fig. 1. In open models it cannot be covered in a similar way, but we can consider only a set of local periodic boxes connected along each light ray, as in Fig. 2. In these boxes we can describe the evolution in the distribution of particles in terms of local flat coordinates $\bar{\mathbf{y}}$, because the size of boxes is much smaller than the curvature radius.

The time evolution in the distribution of particles was derived by performing the N -body simulation in the tree-code provided by Suto. The initial particle distributions were derived using Bertschinger's software *COSMICS*⁶⁾ under the condition

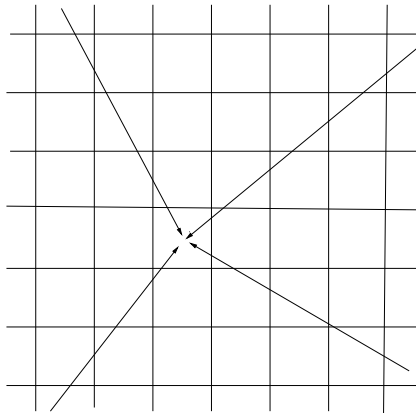


Fig. 1. Light rays and periodic boxes in the flat space.

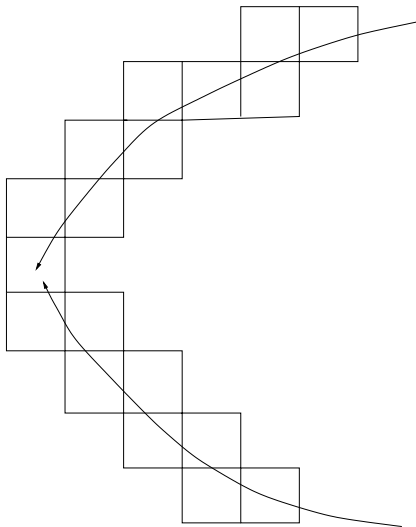


Fig. 2. Light rays and local periodic boxes shown schematically in a curved space.

that their perturbations are given as random fields with the spectrum of cold dark matter, their power n is 1, and their normalization is specified as the dispersion $\sigma_8 = 0.94$ with the Hubble constant $h = 0.7$.

For the integration of the above null-geodesic equations, we calculate the potential at a finite number of points on the ray which are given at each time step (ΔT). Then particles near one of the points on the ray have a stronger influence upon the potential than particles far from any points. To avoid this unbalance in the calculation of the potential, we take an average of the potential ϕ_1 by integrating it analytically over the interval between one of the points and the next point. The expression for an averaged potential $\bar{\phi}$ was given in the previous paper. Moreover, to take into account the finite particle size as galaxies or clouds, we modify the above potential for point sources using the softening radii $y_s = a(t_1)x_s/R$. The modified potential is produced by replacing $(y - y_n)^2$ to $(y - y_s)^2 + (y_s)^2$ in the potential for

point sources.

The initial values of \tilde{K}^i are given so as to satisfy Eq. (2.16). The integration of Eqs. (2.13) and (2.14) with the modified potential was performed using the Adams method as in our previous papers. As the time step we assumed $\Delta T = [\ln 6/2]/N_s$ with $/N_s = 3000$ (in most cases) -10000 .

§3. Statistical behavior of optical quantities

We treat the deformation of ray bundles over the interval from $z = 0$ to $z = 5$ measured by an observer in a periodic box. In the same way as in the previous paper⁴⁾, we consider here the ray bundles reaching the observer in a regular form such that the rays are put in the same separation angle θ , and calculate the change in the angular positions of the rays increasing with redshift in the past direction. From this change we find the behavior of optical quantities.

Basic ray bundles consist of 5×5 rays which are put in the square form with the same separation angle $\theta = 2 - 360$ arcsec. Many bundles coming from all directions in the sky are considered. Here we take 200 bundles coming from randomly chosen directions for each separation angle. In order to express angular positions of rays, we use two orthogonal vectors $e_{(1)}^i$ and $e_{(2)}^i$ in the plane perpendicular to the first background ray vector $(\tilde{K}^i)_B$. Then the angular coordinates $[X(m, n), Y(m, n)]$ of 25 rays relative to the first ray with $(m, n) = (1, 1)$ at any epoch are defined by

$$\begin{aligned} X(m, n) &= \sum_i [y^i(m, n) - y^i(1, 1)] e_{(1)}^i / y_B(1, 1) + X(1, 1), \\ Y(m, n) &= \sum_i [y^i(m, n) - y^i(1, 1)] e_{(2)}^i / y_B(1, 1) + Y(1, 1), \end{aligned} \quad (3.1)$$

where $y^i = y_B^i + \delta y^i$ and $y_B = [\sum_i (y_B^i)^2]$. Since all angular intervals of rays at the observer's point are the same ($= \theta$), differentiation of angular coordinates of the rays at any epoch with respect to those at observer's points is given by the following differences:

$$\begin{aligned} A_{11}(m, n) &= [X(m+1, n) - X(m, n)] / \theta, \\ A_{12}(m, n) &= [X(m, n+1) - X(m, n)] / \theta, \\ A_{21}(m, n) &= [Y(m+1, n) - Y(m, n)] / \theta, \\ A_{22}(m, n) &= [Y(m, n+1) - Y(m, n)] / \theta, \end{aligned} \quad (3.2)$$

where m and n run from 1 to 5. From the matrix $A_{ij}(m, n)$ we derive the optical quantities in the standard manner,⁷⁾ as the convergence ($\kappa(m, n)$), the shear ($\gamma_i(m, n)$, $i = 1, 2$), and the amplification ($\mu(m, n)$) defined by

$$\begin{aligned} \kappa(m, n) &= 1 - \text{tr}(m, n) / 2, \quad \gamma_1(m, n) = [A_{22}(m, n) - A_{11}(m, n)] / 2, \\ \gamma_2(m, n) &= -[A_{12}(m, n) + A_{21}(m, n)] / 2, \\ \gamma^2 &\equiv (\gamma_1)^2 + (\gamma_2)^2 = [\text{tr}(m, n)]^2 - \det(A_{ij}(m, n)), \\ \mu(m, n) &= 1 / \det(A_{ij}(m, n)), \end{aligned} \quad (3.3)$$

The average optical quantities in each bundle are defined as the averages of optical

quantities for all rays in the bundle as follows:

$$\bar{\kappa} = \left[\sum_m \sum_n \kappa(m, n) \right] / 4^2, \quad \bar{\kappa}^2 = \left[\sum_m \sum_n (\kappa(m, n))^2 \right] / 4^2, \quad (3.4)$$

and so on. In this averaging process the contributions from smaller scales can be cancelled and smoothed-out. The above optical quantities at the separation angle θ are accordingly derived in the coarse-graining on this smoothing scale.

For the present statistical analysis we excluded the caustic cases and considered only the cases of weak lensing in the sense of no caustics. The averaging for all non-caustic ray bundles is denoted using $\langle \rangle$ as $\langle \kappa^2 \rangle$, $\langle \gamma^2 \rangle$ and $\langle (\mu - 1)^2 \rangle$. Because $\kappa(m, n)$, $\gamma_i(m, n)$ and $\mu(m, n) - 1$ take positive and negative values with almost equal frequency, $\langle \kappa \rangle$, $\langle \gamma_i \rangle$ and $\langle \mu \rangle - 1$ are small.

In Figs. 3 and 4, we show the behavior of $\langle \kappa^2 \rangle$ and $\langle \gamma^2 \rangle$ for various separation angles $\theta = 2 \text{ arcsec} - 360 \text{ arcsec}$ ($= 6 \text{ arcmin}$). It is found that $\langle \kappa^2 \rangle^{1/2}$ and $\langle \gamma^2 \rangle^{1/2}$ for $\Omega_0 = 0.4$ (model O2) are larger than those for $\Omega_0 = 0.2$ (model O1) at all separation angles $\theta = 2 - 360 \text{ arcsec}$ and the difference Δ is about 0.005 – 0.01 at both periods $z = 1$ and 2, and that for $\Omega_0 = 0.2$ those in the open model (O1) are larger than those in the flat model (L) and their difference Δ' is comparable with the above Δ . The amount of optical quantities for $\theta \sim 360 \text{ arcsec}$ is consistent with the results of Bernardeau et al. (cf. their Figs. 3 and 4)⁸⁾ and Nakamura⁹⁾ in their treatments. The differences of quantities between various cosmological models are closely connected with the differences of angular diameter distances in their models, because for the same separation angle larger angular diameter distances correspond to longer inhomogeneities with smaller amounts and so smaller deformations are brought to rays passing through them. Here let us examine the behavior of angular diameter distances to explain this situation. In weak lensing the Friedmann angular diameter distances can be used approximately to most rays, and their behaviors are shown in Fig.5 for models with $(\Omega_0, \lambda_0) = (1, 0), (0.4, 0), (0.2, 0)$ and $(0.2, 0.8)$. The basic equations for deriving this distances can be seen in a standard text.⁷⁾ From this figure we find that these models stand in inverse order of length of the distances, and so that in model L the distance is larger for equal redshifts and rays with the same separation angles have smaller deformations than in model O1.

In Tables I, II and III, we show for models O1, O2 and L the numerical values of $\langle \kappa \rangle$, $\langle \kappa^2 \rangle^{1/2}$, $\langle \mu \rangle$, $\langle (\mu - 1)^2 \rangle^{1/2}$, $\langle \gamma_1 \rangle$ and $\langle \gamma^2 \rangle^{1/2}$ at epochs $z = 1, 2, \dots, 5$ for $\theta = 2 \text{ arcsec}$.

§4. Concluding remarks

In this paper we assumed that all low-density models (O1, O2 and L) contain only compact lens objects with the same mass and radius, and compared their optical quantities. If we assume that particles in model O2 consist of compact lens objects and clouds with same mass but larger radius and that the number of compact lens objects is equal to that in models O1 and L, the values of optical quantities in model O2 will decrease as the radius of clouds increase, just as S(b) and S(c) in the Einstein-de Sitter model S, which were shown in the previous paper.⁴⁾

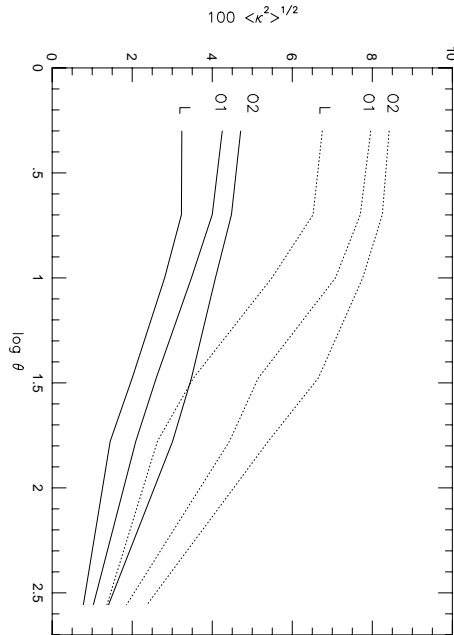


Fig. 3. The angular dependence of $\langle \kappa^2 \rangle^{1/2}$. Solid and dotted lines denote behaviors for $z = 1$ and 2, respectively. The separation angle θ is in the unit of arcsec.

For the statistical analysis we used 200 ray bundles reaching an observer in a single inhomogeneous model universe. This number of ray bundles may be too small to cover the influences from complicated inhomogeneities in all directions. For getting more robust statistical results it may be necessary to use more ray bundles and more model universes produced with random numbers.

Here we touch recent observations of cosmological shear due to weak lensing and their relation to our results. Fort et al.¹⁰⁾ attempted the measurements of a coherent shear from foreground mass condensations in the fields of several luminous radio sources. Schneider et al.¹¹⁾ determined the shear in the field (2 min \times 2 min) containing a radio source PKS1508-05 with $z = 1.2$, and their result is that the shear is about 0.03 for the angular scale 1 min. If we interpret this value as an upper limit of the average shear in the general field due to weak lensing, we find from our result in Fig. 4 that Ω_0 is ~ 0.4 at large. For its more confident estimate, more observational data of coherent shears in various fields are required.

Acknowledgments

The author would like to thank Y. Suto, M. Itoh, and K. Yoshikawa for helpful discussions about N -body simulations. Numerical calculations were performed on the YITP computer system.

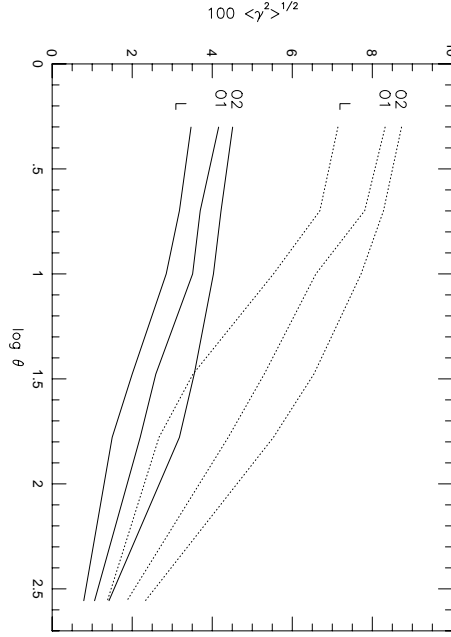


Fig. 4. The angular dependence of $\langle \gamma^2 \rangle^{1/2}$. Solid and dotted lines denote behavior for $z = 1$ and 2, respectively. The separation angle θ is in the unit of arcsec.

Appendix A

— Basic Equations of Null Rays —

Corresponding to the line-element (2.10), we consider first the wave-vectors $K^\mu \equiv (K^0, K^i) = dy^\mu/dv$, where v is an affine parameter. The null condition is

$$\begin{aligned} \mathcal{L} \equiv & -[\Omega_0 + (1 - \Omega_0 - \lambda_0)S + \lambda_0 S^3]^{-1} e^{6T} (1 + \alpha\phi) (K^0)^2 \\ & + c_R^{-2} (1 - \alpha\phi) e^{4T} \sum_i (K^i)^2 / F(\mathbf{y})^2 = 0, \end{aligned} \quad (\text{A.1})$$

where F is defined in Eq.(2.12). From the equation

$$\frac{d}{dv} \frac{\partial \mathcal{L}}{\partial K^\mu} = \frac{\partial \mathcal{L}}{\partial y^\mu}, \quad (\text{A.2})$$

we obtain

$$\begin{aligned} \frac{dK^0}{dv} + \frac{3\Omega_0 + 2(1 - \Omega_0 - \lambda_0)e^{2(T-T_0)}}{G(T)} (K^0)^2 + \frac{2G(T)}{c_R^2 e^{2T} F^2} \sum_i (K^i)^2 \\ + \alpha \left\{ \frac{1}{2} \frac{\partial \phi}{\partial T} \left[(K^0)^2 - G(T) c_R^{-2} e^{-2T} \sum_i (K^i)^2 / F^2 \right] + \frac{\partial \phi}{\partial y^i} K^i K^0 \right\} \end{aligned}$$

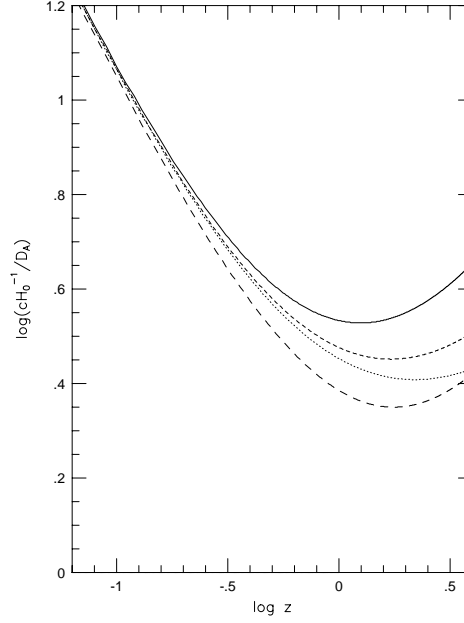


Fig. 5. The z dependence of the angular diameter distance D_A for $\alpha = 1$. Models S(1,0), O1(0.2,0), O2(0.4,0) and L(0.2,0.8) are denoted by solid, dotted, short dashed, long dashed lines, respectively.

$$-2c_R^{-2}e^{-2T}\phi G(T)\sum_i(K^i)^2/F^2\} = 0, \quad (\text{A}\cdot 3)$$

$$\begin{aligned} \frac{dK^i}{dv} + \left(4 - \alpha \frac{\partial \phi}{\partial T}\right) K^0 K^i - \alpha \frac{\partial \phi}{\partial y^j} K^i K^j \\ + \frac{1}{2} \alpha \frac{\partial \phi}{\partial y^i} \left[c_R^2 e^{2T} G^{-1}(T) (K^0)^2 + \sum_l (K^l)^2 / F^2 \right] \\ + (R_0 H_0 / c)^2 (1 - \Omega_0 - \lambda_0) F^{-1} \left[\sum_l y^l K^l K^i - \frac{1}{2} \sum_l (K^l)^2 y^i \right] = 0, \end{aligned} \quad (\text{A}\cdot 4)$$

where $G(T)$ is defined by Eq. (2.15).

Transforming v to T , these equations lead to

$$\frac{dK^0}{dT} + \left[\frac{3\Omega_0 + 2(1 - \Omega_0 - \lambda_0)e^{2(T-T_0)}}{G(T)} + 2 \right] K^0 + \alpha \frac{\partial \phi}{\partial y^i} K^i = 0, \quad (\text{A}\cdot 5)$$

$$\begin{aligned} \frac{dK^i}{dT} + \left(4 - \alpha \frac{\partial \phi}{\partial T}\right) K^i - \alpha \frac{\partial \phi}{\partial y^j} \frac{K^j K^i}{K^0} + e^{2T} (c_R)^2 G^{-1}(T) \frac{\alpha \partial \phi}{\partial y^i} \\ + (R_0 H_0 / c)^2 (1 - \Omega_0 - \lambda_0) F^{-1} \left[\sum_j y^j K^j K^i / K^0 \right] \end{aligned}$$

$$-\frac{1}{2}e^{2T}(c_R)^2G^{-1}(T)(1+2\alpha\phi)y^iK^0] = 0. \quad (\text{A}\cdot 6)$$

Moreover, if we use for K^i

$$\tilde{K}^i \equiv c_R^{-1}e^{-T}K^i/K^0, \quad (\text{A}\cdot 7)$$

we obtain Eqs. (2.13) and (2.14).

References

- [1] R.D. Blandford, A. Saust, T. Brainerd, J. Villumsen, *Month. Notices. Astron. Soc.* **251** (1991), 600
- [2] J. Villmsen, *Month. Notices. Astron. Soc.* **281** (1996), 369
- [3] P. Schneider, L. van Waerbeke, B. Jain, and G. Kruse, *astro-ph/9708143*
- [4] K. Tomita, *Prog. Theor. Phys.* **99** (1998), 97
- [5] Y. Suto, *Prog. Theor. Phys.* **90** (1993), 1173
- [6] E. Bertschinger, *astro-ph/9506070*
- [7] P. Schneider, J. Ehlers and E. E. Falco, *Gravitational Lenses* (Springer-Verlag, New York, 1992)
- [8] F. Bernardeau, L. Van Waerbeke and Y. Mellier, *Astron. Astrophys.* **322** (1997), 1
- [9] T.T. Nakamura, *Publ. Astron. Soc. Japan* **49** (1997), 151
- [10] B. Ford, Y. Miller, M. Dantel-Fort, H. Bonnet, and J.-P. Kneib, *Astron. Astrophys.* **310** (1996), 705
- [11] P. Schneider, L. van Waerbeke, Y. Miller, B. Jain, S. Seits and B. Ford, *astro-ph/9705122*

Table I. Optical quantities in model O1.

z	$\langle \kappa \rangle$	$\langle \kappa^2 \rangle^{1/2}$	$\langle \mu \rangle$	$\langle (1-\mu)^2 \rangle^{1/2}$	$\langle \gamma_1 \rangle$	$\langle \gamma^2 \rangle^{1/2}$
1	-0.0002	0.0425	1.0221	0.1219	-0.0028	0.0426
2	-0.0054	0.0796	0.9961	0.2210	-0.0041	0.0832
3	-0.0069	0.1157	1.0368	0.6234	0.0057	0.1225
4	-0.0081	0.1519	1.0790	0.5638	0.0078	0.1602
5	-0.0064	0.1872	1.1627	1.1880	0.0120	0.1980

Table II. Optical quantities in model O2.

z	$\langle \kappa \rangle$	$\langle \kappa^2 \rangle^{1/2}$	$\langle \mu \rangle$	$\langle (1-\mu)^2 \rangle^{1/2}$	$\langle \gamma_1 \rangle$	$\langle \gamma^2 \rangle^{1/2}$
1	0.0008	0.0471	1.0126	0.1305	-0.0011	0.0451
2	0.0071	0.0842	1.0517	0.2755	-0.0001	0.0873
3	0.0111	0.1103	1.0980	0.4956	-0.0022	0.1255
4	0.0136	0.1380	1.1602	1.0742	-0.0019	0.1613
5	0.0147	0.1680	1.1926	1.5755	-0.0028	0.1958

Table III. Optical quantities in model L.

z	$\langle \kappa \rangle$	$\langle \kappa^2 \rangle^{1/2}$	$\langle \mu \rangle$	$\langle (1-\mu)^2 \rangle^{1/2}$	$\langle \gamma_1 \rangle$	$\langle \gamma^2 \rangle^{1/2}$
1	-0.0011	0.0324	1.0025	0.0705	0.0008	0.0347
2	-0.0036	0.0675	1.0134	0.1572	0.0018	0.0714
3	-0.0045	0.0974	1.0345	0.2407	0.0020	0.1002
4	-0.0065	0.1216	1.0560	0.3209	0.0023	0.1214
5	-0.0070	0.1405	1.0805	0.4000	0.0030	0.1372